第二十一届全国重味物理和CP破坏研讨会

Light single-gluon hybrid states with various exotic quantum numbers

Wei-Han Tan

Southeast University

Collaborator:Niu Su, Hua-Xing Chen,Shi-Lin Zhu,Wei Chen

Outline

- Introduction
- Method of the QCD sum rules
- Numerical analyses
- Decay behavior
- Summary

Outline

- Introduction
- Method of the QCD sum rules
- Numerical analyses
- Decay behavior
- Summary

Introduction

- **Traditional quark model**

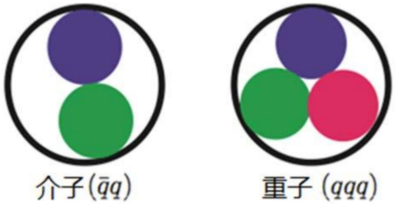

- **Exotic hadron: hybrid state, glueball, tetraquark, etc.**

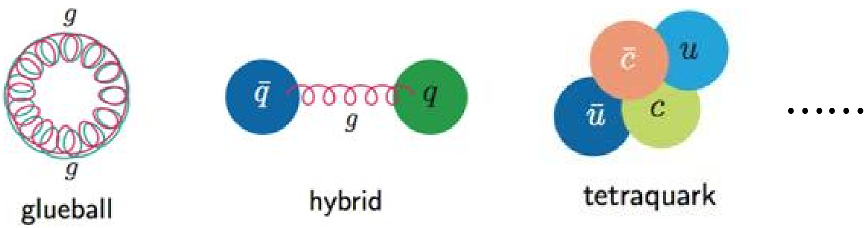

- **Exotic spin-parity quantum numbers**

$$0^{--}, 0^{+-}, 1^{-+}, 2^{+-}$$

Introduction

BESIII

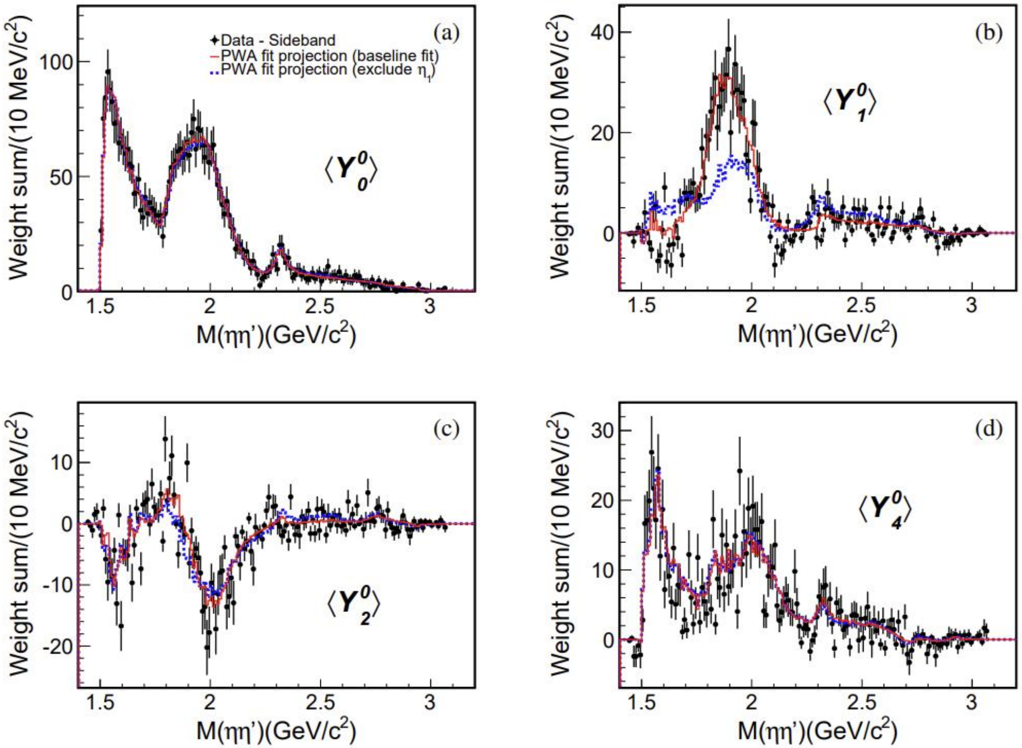

FIG. 3. The distributions of the unnormalized moments $\langle Y_L^0 \rangle$ ($L = 0$, 1, 2, and 4) for $J/\psi \to \gamma\eta\eta'$ as functions of the $\eta\eta'$ mass. Black dots with error bars represent the background-subtracted data weighted with angular moments; the red solid lines represent the baseline fit projections; and the blue dotted lines represent the projections from a fit excluding the η_1 component.

M. Ablikim, et al., Observation of an Isoscalar Resonance with Exotic $J^{PC} = 1^{-+}$ Quantum Numbers in J/ψ → γηη ′ , Phys. Rev. Lett. 129 (19) (2022) 192002. arXiv:2202.00621, doi:10.1103/ PhysRevLett.129.192002.

$$\eta_1(1855) \ : \ M = 1855 \pm 9^{+6}_{-1} \ \mathrm{MeV}/c^2 \,,$$
$$\Gamma = 188 \pm 18^{+3}_{-8} \ \mathrm{MeV} \,.$$

Introduction

$$\eta_1(1855) \ : \ M = 1855 \pm 9^{+6}_{-1} \ \mathrm{MeV}/c^2 \,,$$
$$\Gamma = 188 \pm 18^{+3}_{-8} \ \mathrm{MeV} \,.$$

$$\pi_1(1400) \ : \ M = 1354 \pm 25 \ \mathrm{MeV} \,,$$
$$\Gamma = 330 \pm 35 \ \mathrm{MeV} \,;$$
$$\pi_1(1600) \ : \ M = 1661^{+15}_{-11} \ \mathrm{MeV} \,,$$
$$\Gamma = 240 \pm 50 \ \mathrm{MeV} \,;$$
$$\pi_1(2015) \ : \ M = 2014 \pm 20 \pm 16 \ \mathrm{MeV} \,,$$
$$\Gamma = 230 \pm 32 \pm 73 \ \mathrm{MeV} \,.$$

Introduction

$$m_{\pi_1(1400)} = 1351 \pm 30\text{MeV}$$

H.-C. Kim, Y. Kim, JHEP 01 (2009) 034. arXiv:0811. 0645, doi:10.1088/1126-6708/2009/01/034.

$$m_{\pi_1(1600)} = 1980 \pm 21\text{MeV}$$

Juzheng Liang, Siyang Chen, Ying Chen, Chunjiang Shi, Wei Sun (2024). arXiv:hep-lat/2409.14410v1.

$$m_{1^{-+}} = 2110\text{MeV}$$

C. McNeile, C. W. Bernard, T. A. DeGrand, C. E. DeTar, S. A. Gottlieb, U. M. Heller, J. Hetrick, R. Sugar, D. Toussaint, Nucl. Phys. B Proc. Suppl. 73 (1999) 264–266. arXiv:hep-lat/ 9809087, doi:10.1016/S0920-5632(99)85043-9.

Introduction

- The QCD sum rule method has been widely applied to study the $J^{PC} = 1^{-+}$ hybrid states.

  Nucl. Phys. B 248 (1984) 1–18.Phys. Lett. B 485 (2000) 145–150
  Eur.Phys. J. C 8 (1999) 465–471. Z.Phys. C 34 (1987) 347.
  Phys. Rev. D 76(2007) 094001. Nucl. Phys. B 196 (1982) 125–146.
  Phys. Lett.B 675 (2009) 319–325.

- This method has also been applied to study the $J^{PC} = 0^{+-}$ and 2^{+-} hybrid states.

  Phys. Rev. D 98 (9) (2018) 096020. Phys. Rev. D 108(2023), 114010

- The light single-gluon hybrid states with other quantum numbers have not been well studied in the literature. Accordingly, in this paper we shall systematically investigate the single-gluon hybrid states with various (exotic) quantum numbers through the QCD sum rule method.

Outline

- Introduction
- **Method of the QCD sum rules**
- Numerical analyses
- Decay behavior
- Summary

QCD sum rules

- In QCD sum rule analyses, we consider two-point correlation functions:

$$\begin{aligned} & \Pi^{\mu\nu}_{1^{-+}}(q^2) \\ \equiv\ & i\int d^4x e^{iqx}\langle 0|\mathbf{T}[J^{\mu}_{1^{-+}}(x) J^{\nu\dagger}_{1^{-+}}(0)]|0\rangle \\ =\ & (g^{\mu\nu} - q^\mu q^\nu/q^2)\,\Pi_{1^{-+}}(q^2) + (q^\mu q^\nu/q^2)\,\Pi_{0^{++}}(q^2)\,. \end{aligned} \tag{39}$$

where J is the current which can couple to hadronic states.

- We use the dispersion relation to express $\prod_{1^{-+}}(q^2)$ as

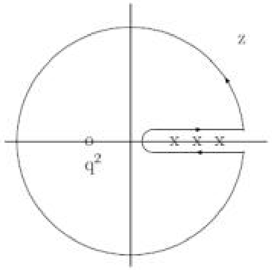

$$\Pi_{1^{-+}}(q^2) = \int_{s_<}^{\infty} \frac{\rho_{1^{-+}}(s)}{s - q^2 - i\varepsilon} ds\,,$$

where $\rho_{1^{-+}}(s) \equiv \mathrm{Im} \prod_{1^{-+}}(s)/\pi$ is the spectral density, and $s_< = 4m_q^2$ is the physical threshold.

QCD sum rules

- At the hadron level, one pole dominance + continuum contribution:

$$
\begin{aligned}
& \rho^{\rm phen}_{1^{-+}}(s) \times (g^{\mu\nu} - q^\mu q^\nu / q^2) \qquad (42) \\
\equiv & \sum_n \delta(s - M_n^2) \langle 0 | J^\mu_{1^{-+}} | n \rangle \langle n | J^{\nu\dagger}_{1^{-+}} | 0 \rangle \\
= & f^2_{1^{-+}} \delta(s - M^2_{1^{-+}}) \times (g^{\mu\nu} - q^\mu q^\nu / q^2) + \text{continuum} \, .
\end{aligned}
$$

- At the quark-gluon level, operator product expansion (OPE). And Borel transformation at both the hadron and quark-gluon levels.

$$
\begin{aligned}
\Pi_{1^{-+}}(s_0, M_B^2) & \equiv f^2_{1^{-+}} e^{-M^2_{1^{-+}}/M_B^2} \\
& = \int_{s_<}^{s_0} e^{-s/M_B^2} \rho^{\rm OPE}_{1^{-+}}(s) ds ,
\end{aligned}
$$

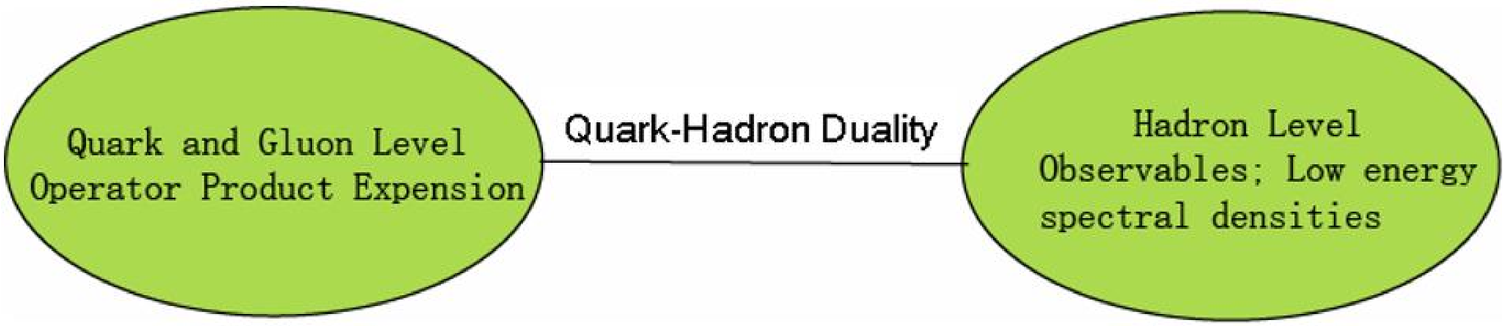

QCD sum rules

$$M^2_{1^{-+}}(s_0, M_B) = \frac{\int_{s_<}^{s_0} e^{-s/M_B^2} s \rho^{\rm OPE}_{1^{-+}}(s) ds}{\int_{s_<}^{s_0} e^{-s/M_B^2} \rho^{\rm OPE}_{1^{-+}}(s) ds}, \quad (44)$$

$$f^2_{1^{-+}}(s_0, M_B) = \Pi_{1^{-+}}(s_0, M_B^2) \times e^{M^2_{1^{-+}}/M_B^2}. \quad (45)$$

- Two parameters： M_B , s_0

- Criteria：

1. Positivity of spectral density
2. Convergence of OPE
3. Sufficient amount of pole contribution
4. The dependence of mass on parameters M_B , s_0

Outline

- Introduction
- Method of the QCD sum rules
- **Numerical analyses**
- Decay behavior
- Summary

Numerical analyses

Interpolating currents:

$$J^{\mu}_{1^{-+}} = \bar{q}_a \lambda_n^{ab} \gamma_\beta q_b \; g_s G_n^{\mu\beta} \, ,$$

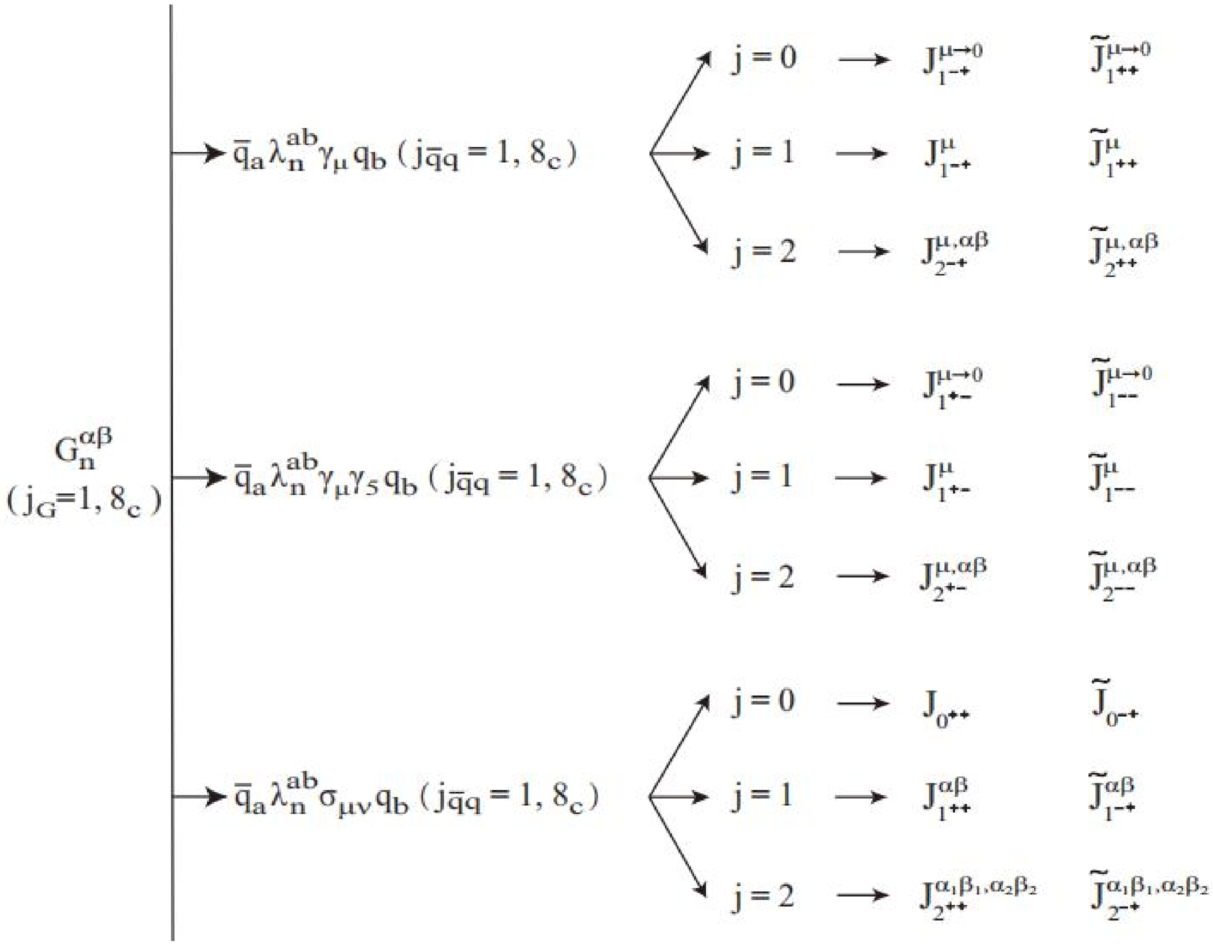

Numerical analyses

The OPE of current $J^{\mu}_{1^{-+}}$

$$\Pi^{\mu}_{1^{-+}}(M_B^2, s_0) = \int_{4m_s^2}^{s_0} \Big(\frac{s^3\alpha_s}{60\pi^3} - \frac{m_s^2 s^2 \alpha_s}{3\pi^3} + s\big(\frac{\langle\alpha_s GG\rangle}{36\pi^2} + \frac{13\langle\alpha_s GG\rangle\alpha_s}{432\pi^3} + \frac{8m_s\langle\bar{s}s\rangle\alpha_s}{9\pi}\big)$$
$$+ \frac{\langle g_s^3 G^3\rangle}{32\pi^2} - \frac{3\langle\alpha_s GG\rangle m_s^2\alpha_s}{64\pi^3} - \frac{3m_s\langle g_s\bar{s}\sigma Gs\rangle\alpha_s}{4\pi}\Big) \times e^{-s/M_B^2} ds$$
$$+ \Big(\frac{\langle\alpha_s GG\rangle^2}{3456\pi^2} - \frac{\langle g_s^3 G^3\rangle m_s^2}{16\pi^2} - \frac{2}{9}\langle\alpha_s GG\rangle m_s\langle\bar{s}s\rangle + \frac{11}{9}\pi\langle\bar{s}s\rangle\langle g_s\bar{s}\sigma Gs\rangle\alpha_s\Big),$$

The OPE with the quark-gluon content $\bar{q}qg$ ($q = u/d$) can be easily derived by replacing $m_s \to 0$, $\langle\bar{s}s\rangle \to \langle\bar{q}q\rangle$, and $\langle g\bar{s}\sigma Gs\rangle \to \langle g\bar{q}\sigma Gq\rangle$.

Numerical analyses

- **Convergence of OPE**

$$\mathrm{CVG}_A \equiv \left| \frac{\Pi^{g_s^{n=4}}(\infty, M_B^2)}{\Pi(\infty, M_B^2)} \right| \leq 5\% \,,$$

$$\mathrm{CVG}_B \equiv \left| \frac{\Pi^{\mathrm{D}=6+8}(\infty, M_B^2)}{\Pi(\infty, M_B^2)} \right| \leq 10\% \,.$$

- **Sufficient amout of pole contribution**

$$\mathrm{PC} \equiv \left| \frac{\Pi(s_0, M_B^2)}{\Pi(\infty, M_B^2)} \right| \geq 40\% \,.$$

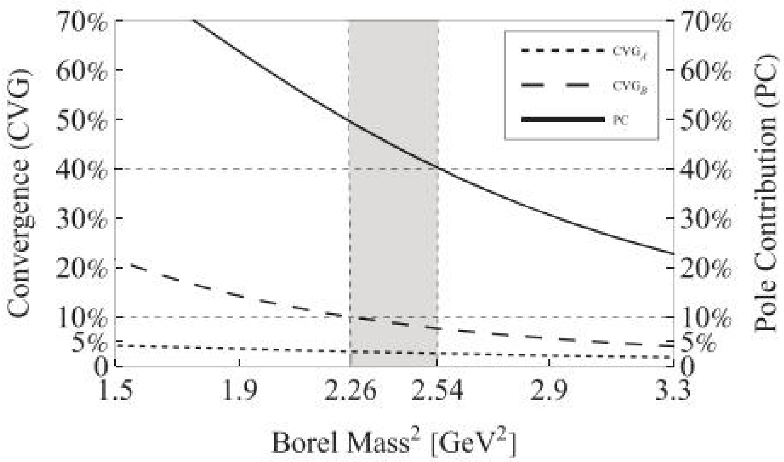

$$2.26\mathrm{GeV}^2 \leq M_B^2 \leq 2.54\mathrm{GeV}^2$$

Note that this Borel window is not so wide, and it may indicate that the understanding of this state as a particle has limitations

Numerical analyses

The dependence of mass on parameters

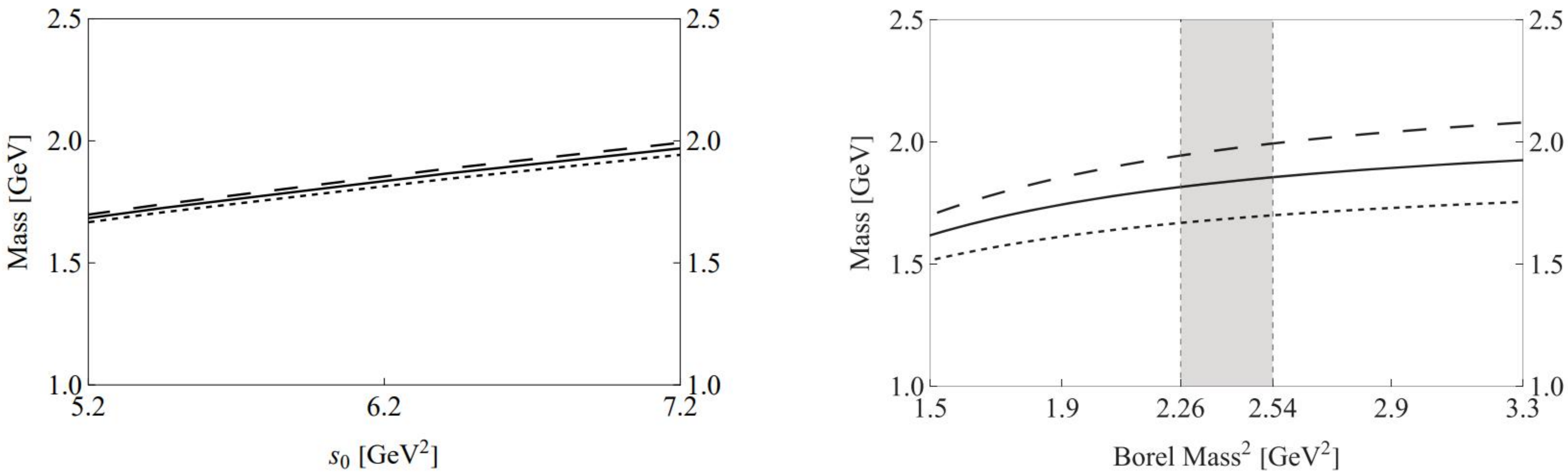

FIG. 4: Mass of the single-gluon hybrid state $|\bar{s}sg;1^{-+}\rangle$ with respect to the threshold value s_0 (left) and the Borel mass M_B (right). In the left panel the dotted, solid, and dashed curves are obtained by setting $M_B^2 = 2.26$ GeV^2, 2.40 GeV^2, and 2.54 GeV^2, respectively. In the right panel the dotted, solid, and dashed curves are obtained by setting $s_0 = 5.2$ GeV^2, 6.2 GeV^2, and 7.2 GeV^2, respectively. These curves are obtained using the spectral density $\rho^{\bar{s}sg}_{1^{-+}}(s)$ extracted from the current $J^{\mu}_{1^{-+}}$ with the quark-gluon content $\bar{s}sg$.

$$M_{|\bar{s}sg;0^+1^{-+}\rangle} = 1.84^{+0.14}_{-0.15}\ \text{GeV}$$

Numerical analyses

Mass extracted from currents of $\bar{s}sg$

State $[J^{PC}]$	Current	s_0^{min} [GeV^2]	Working Regions		Pole [%]	Mass [GeV]	Decay Constant
			M_B^2 [GeV^2]	s_0 [GeV^2]			
$\|\bar{s}sg; 1^{--}\rangle$	$J_{1--}^{\alpha\beta}$	4.3	2.07–2.80	6.5	40–63	$1.94^{+0.20}_{-0.21}$	$0.054^{+0.013}_{-0.016}$ GeV^3
$\|\bar{s}sg; 1^{+-}\rangle$	$\tilde{J}_{1+-}^{\alpha\beta}$	16.2	3.60–5.40	20.0	40–65	$4.06^{+0.26}_{-0.16}$	$0.071^{+0.019}_{-0.020}$ GeV^3
$\|\bar{s}sg; 1^{+-}\rangle$	$J_{1+-}^{\alpha\beta}$	5.9	2.54–2.72	6.5	40–45	$2.01^{+0.17}_{-0.20}$	$0.050^{+0.005}_{-0.006}$ GeV^3
$\|\bar{s}sg; 1^{--}\rangle$	$\tilde{J}_{1--}^{\alpha\beta}$	16.9	3.73–5.30	20.0	40–61	$4.12^{+0.26}_{-0.13}$	$0.070^{+0.019}_{-0.020}$ GeV^3
$\|\bar{s}sg; 0^{++}\rangle$	$J_{1-+}^{\mu\to 0}$	20.7	5.18–7.35	26.0	40–63	$4.50^{+0.23}_{-0.22}$	$0.136^{+0.030}_{-0.034}$ GeV^3
$\|\bar{s}sg; 0^{-+}\rangle$	$\tilde{J}_{1++}^{\mu\to 0}$	7.2	3.45–4.08	9.5	40–53	$2.26^{+0.21}_{-0.24}$	$0.107^{+0.007}_{-0.005}$ GeV^3
$\|\bar{s}sg; 0^{--}\rangle$	$J_{1+-}^{\mu\to 0}$	21.6	5.36–7.23	26.0	40–59	$4.57^{+0.22}_{-0.19}$	$0.134^{+0.031}_{-0.035}$ GeV^3
$\|\bar{s}sg; 0^{+-}\rangle$	$\tilde{J}_{1--}^{\mu\to 0}$	7.5	3.41–3.98	9.5	40–52	$2.30^{+0.20}_{-0.24}$	$0.101^{+0.007}_{-0.006}$ GeV^3
$\|\bar{s}sg; 1^{-+}\rangle$	J_{1-+}^{μ}	5.1	2.26–2.54	6.2	40–49	$1.84^{+0.14}_{-0.15}$	$0.300^{+0.063}_{-0.058}$ GeV^4
$\|\bar{s}sg; 1^{++}\rangle$	$\tilde{J}_{1++}^{\mu}$	14.1	3.64–4.80	17.0	40–58	$3.65^{+0.17}_{-0.17}$	$1.678^{+0.530}_{-0.502}$ GeV^4
$\|\bar{s}sg; 1^{+-}\rangle$	J_{1+-}^{μ}	3.9	1.85–2.43	6.0	40–62	$1.82^{+0.13}_{-0.15}$	$0.278^{+0.059}_{-0.056}$ GeV^4
$\|\bar{s}sg; 1^{--}\rangle$	$\tilde{J}_{1--}^{\mu}$	13.8	3.50–4.80	17.0	40–61	$3.64^{+0.17}_{-0.17}$	$1.662^{+0.526}_{-0.498}$ GeV^4

Numerical analyses

State $[J^{PC}]$	Current	s_0^{min} [GeV^2]	Working Regions M_B^2 [GeV^2]	Working Regions s_0 [GeV^2]	Pole [%]	Mass [GeV]	Decay Constant
$\lvert\bar{s}sg;0^{++}\rangle$	J_{0++}	11.5	3.53–4.33	14.0	40–55	$3.11^{+0.22}_{-0.27}$	$3.535^{+1.338}_{-1.242}$ GeV^4
$\lvert\bar{s}sg;0^{-+}\rangle$	J_{0-+}	11.3	3.51–4.36	14.0	40–56	$3.08^{+0.23}_{-0.28}$	$3.509^{+1.328}_{-1.233}$ GeV^4
$\lvert\bar{s}sg;1^{++}\rangle$	$J^{\alpha\beta}_{1++}$	6.6	1.95–2.27	7.5	40–51	$2.34^{+0.14}_{-0.16}$	$0.061^{+0.012}_{-0.014}$ GeV^3
$\lvert\bar{s}sg;1^{-+}\rangle$	$\tilde{J}^{\alpha\beta}_{1-+}$	5.5	1.82–2.25	7.0	40–57	$2.08^{+0.18}_{-0.24}$	$0.061^{+0.010}_{-0.010}$ GeV^3
$\lvert\bar{s}sg;1^{-+}\rangle$	$J^{\alpha\beta}_{1-+}$	5.5	1.82–2.25	7.0	40–57	$2.08^{+0.18}_{-0.24}$	$0.061^{+0.010}_{-0.010}$ GeV^3
$\lvert\bar{s}sg;1^{++}\rangle$	$\tilde{J}^{\alpha\beta}_{1++}$	6.6	1.95–2.27	7.5	40–51	$2.34^{+0.14}_{-0.16}$	$0.061^{+0.012}_{-0.014}$ GeV^3
$\lvert\bar{s}sg;2^{++}\rangle$	$J^{\alpha_1\beta_1,\alpha_2\beta_2}_{2++}$	9.2	3.22–3.60	10.5	40–49	$2.59^{+0.19}_{-0.23}$	–
$\lvert\bar{s}sg;2^{-+}\rangle$	$\tilde{J}^{\alpha_1\beta_1,\alpha_2\beta_2}_{2-+}$	13.4	2.55–4.29	16.0	40–66	$3.72^{+0.72}_{-0.13}$	–
$\lvert\bar{s}sg;2^{-+}\rangle$	$J^{\alpha_1\beta_1,\alpha_2\beta_2}_{2-+}$	8.1	3.04–3.72	10.5	40–56	$2.51^{+0.20}_{-0.24}$	–
$\lvert\bar{s}sg;2^{++}\rangle$	$\tilde{J}^{\alpha_1\beta_1,\alpha_2\beta_2}_{2++}$	11.8	2.36–4.47	16.0	40–78	$3.54^{+0.42}_{-0.16}$	–

$$M_{|\bar{s}sg;0^+1^{-+}\rangle} = 1.84^{+0.14}_{-0.15}\ \text{GeV}\,,$$
$$f_{|\bar{s}sg;0^+1^{-+}\rangle} = 0.300^{+0.063}_{-0.058}\ \text{GeV}^4$$

Numerical analyses

Mass extracted from currents of $\bar{q}qg(q = u/d)$

State $[J^{PC}]$	Current	s_0^{min} [GeV^2]	Working Regions M_B^2 [GeV^2]	Working Regions s_0 [GeV^2]	Pole [%]	Mass [GeV]	Decay Constant
$\|\bar{q}qg;1^{--}\rangle$	$J^{\alpha\beta}_{1--}$	4.2	2.03–2.48	5.5	40–54	$1.80^{+0.13}_{-0.16}$	$0.051^{+0.004}_{-0.004}$ GeV^3
$\|\bar{q}qg;1^{+-}\rangle$	$\tilde{J}^{\alpha\beta}_{1+-}$	16.2	3.61–4.58	18.0	40–53	$4.05^{+0.24}_{-0.12}$	$0.063^{+0.020}_{-0.020}$ GeV^3
$\|\bar{q}qg;1^{+-}\rangle$	$J^{\alpha\beta}_{1+-}$	5.0	2.29–2.45	5.5	40–45	$1.84^{+0.12}_{-0.14}$	$0.049^{+0.004}_{-0.004}$ GeV^3
$\|\bar{q}qg;1^{--}\rangle$	$\tilde{J}^{\alpha\beta}_{1--}$	16.3	3.52–4.56	18.0	40–53	$4.09^{+0.29}_{-0.14}$	$0.064^{+0.021}_{-0.020}$ GeV^3
$\|\bar{q}qg;0^{++}\rangle$	$J^{\mu\to 0}_{1-+}$	20.6	5.11–6.59	24.0	40–56	$4.45^{+0.22}_{-0.17}$	$0.124^{+0.032}_{-0.036}$ GeV^3
$\|\bar{q}qg;0^{-+}\rangle$	$\tilde{J}^{\mu\to 0}_{1++}$	7.7	3.58–3.81	8.5	40–45	$2.14^{+0.17}_{-0.19}$	$0.105^{+0.005}_{-0.004}$ GeV^3
$\|\bar{q}qg;0^{--}\rangle$	$J^{\mu\to 0}_{1+-}$	21.6	5.48–6.52	24.0	40–50	$4.49^{+0.21}_{-0.14}$	$0.123^{+0.032}_{-0.037}$ GeV^3
$\|\bar{q}qg;0^{+-}\rangle$	$\tilde{J}^{\mu\to 0}_{1--}$	7.1	3.32–3.73	8.5	40–49	$2.16^{+0.16}_{-0.19}$	$0.100^{+0.005}_{-0.005}$ GeV^3
$\|\bar{q}qg;1^{-+}\rangle$	J^{μ}_{1-+}	4.8	2.19–2.28	5.2	40–43	$1.67^{+0.15}_{-0.17}$	$0.243^{+0.057}_{-0.052}$ GeV^4
$\|\bar{q}qg;1^{++}\rangle$	$\tilde{J}^{\mu}_{1++}$	13.8	3.59–4.10	15.0	40–48	$3.54^{+0.16}_{-0.12}$	$1.370^{+0.494}_{-0.450}$ GeV^4
$\|\bar{q}qg;1^{+-}\rangle$	J^{μ}_{1+-}	4.6	2.10–2.27	5.2	40–46	$1.68^{+0.14}_{-0.16}$	$0.242^{+0.055}_{-0.051}$ GeV^4
$\|\bar{q}qg;1^{--}\rangle$	$\tilde{J}^{\mu}_{1--}$	13.7	3.57–4.10	15.0	40–49	$3.53^{+0.16}_{-0.12}$	$1.366^{+0.493}_{-0.450}$ GeV^4

Numerical analyses

State $[J^{PC}]$	Current	s_0^{min} [GeV^2]	Working Regions M_B^2 [GeV^2]	s_0 [GeV^2]	Pole [%]	Mass [GeV]	Decay Constant
$\|\bar{q}qg;0^{++}\rangle$	J_{0++}	11.1	3.48–3.91	12.5	40–49	$2.94^{+0.20}_{-0.25}$	$2.893^{+1.029}_{-0.948}$ GeV^4
$\|\bar{q}qg;0^{-+}\rangle$	J_{0-+}	11.1	3.47–3.92	12.5	40–49	$2.93^{+0.20}_{-0.25}$	$2.882^{+1.026}_{-0.945}$ GeV^4
$\|\bar{q}qg;1^{++}\rangle$	$J^{\alpha\beta}_{1++}$	5.8	1.84–2.06	6.5	40–48	$2.11^{+0.17}_{-0.21}$	$0.056^{+0.012}_{-0.013}$ GeV^3
$\|\bar{q}qg;1^{-+}\rangle$	$\tilde{J}^{\alpha\beta}_{1-+}$	5.5	1.81–2.00	6.2	40–48	$2.00^{+0.13}_{-0.16}$	$0.055^{+0.007}_{-0.008}$ GeV^3
$\|\bar{q}qg;1^{-+}\rangle$	$J^{\alpha\beta}_{1-+}$	5.5	1.81–2.00	6.2	40–48	$2.00^{+0.13}_{-0.16}$	$0.055^{+0.007}_{-0.008}$ GeV^3
$\|\bar{q}qg;1^{++}\rangle$	$\tilde{J}^{\alpha\beta}_{1++}$	5.8	1.84–2.06	6.5	40–48	$2.11^{+0.17}_{-0.21}$	$0.056^{+0.012}_{-0.013}$ GeV^3
$\|\bar{q}qg;2^{++}\rangle$	$J^{\alpha_1\beta_1,\alpha_2\beta_2}_{2++}$	8.6	3.11–3.37	9.5	40–46	$2.44^{+0.20}_{-0.24}$	–
$\|\bar{q}qg;2^{-+}\rangle$	$\tilde{J}^{\alpha_1\beta_1,\alpha_2\beta_2}_{2-+}$	12.7	2.54–3.60	14.0	40–54	$3.68^{+0.62}_{-0.18}$	–
$\|\bar{q}qg;2^{-+}\rangle$	$J^{\alpha_1\beta_1,\alpha_2\beta_2}_{2-+}$	8.3	3.07–3.41	9.5	40–48	$2.40^{+0.21}_{-0.25}$	–
$\|\bar{q}qg;2^{++}\rangle$	$\tilde{J}^{\alpha_1\beta_1,\alpha_2\beta_2}_{2++}$	11.7	2.47–3.70	14.0	40–63	$3.46^{+0.27}_{-0.11}$	–

$$M_{|\bar{q}qg;1^-1^{-+}\rangle} = M_{|\bar{q}qg;0^+1^{-+}\rangle} = 1.67^{+0.15}_{-0.17}\ \text{GeV}\,,$$
$$f_{|\bar{q}qg;1^-1^{-+}\rangle} = f_{|\bar{q}qg;0^+1^{-+}\rangle} = 0.243^{+0.057}_{-0.052}\ \text{GeV}^4$$

Outline

- Introduction
- Method of the QCD sum rules
- Numerical analyses
- **Decay behavior**
- Summary

Decay behavior

Decay processes: normal & abnormal

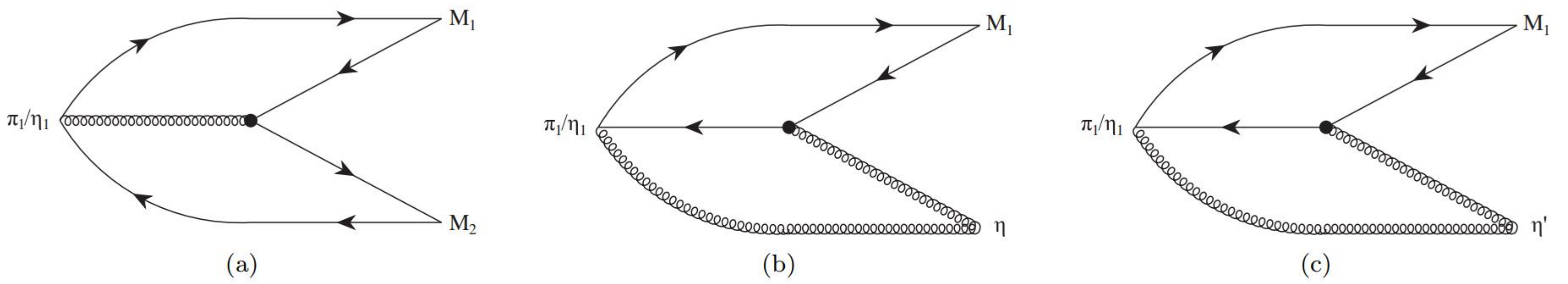

FIG. 5: Decay mechanisms of the single-gluon hybrid states through (a) the normal process with one quark-antiquark pair excited from the valence gluon, and (b,c) the abnormal processes with the η/η' produced by the QCD axial anomaly.

A. Normal decay process

three-point correlation function:

$$\pi_1 \equiv |\bar{q}qg; 1^-1^{-+}\rangle \to \rho\pi\,,$$

$$T_{\mu\nu}(p,k,q) = \int d^4x d^4y e^{ikx} e^{iqy} \times \langle 0|\mathbb{T}[J_\nu^{\rho^-}(x) J_5^{\pi^+}(y) J_{1^{-+}}^{\mu\dagger}(0)]|0\rangle$$

Decay behavior

select the isovector neutral-charged one

$$J^{\mu}_{1^{-+}} \to \frac{1}{\sqrt{2}} \left(\bar{u}_a \lambda_n^{ab} \gamma_\beta u_b - \bar{d}_a \lambda_n^{ab} \gamma_\beta d_b \right) g_s G_n^{\mu\beta}$$

phenomenological side

$$T_{\mu\nu}(p,k,q) = g_{\rho\pi} \epsilon_{\mu\nu\alpha\beta} q^\alpha k^\beta \times \frac{f_{\pi_1} f_\rho m_\rho f'_\pi}{(m^2_{\pi_1} - p^2)(m^2_\rho - k^2)(m^2_\pi - q^2)}$$

QCD side

$$T_{\mu\nu}(p,k,q) = \frac{\epsilon_{\mu\nu\alpha\beta} q^\alpha k^\beta}{q^2} \times \quad (65)$$

$$\left(\frac{\langle g_s \bar{q} \sigma G q \rangle}{6\sqrt{2}} \left(\frac{3}{p^2} + \frac{1}{k^2} \right) - \frac{\langle \bar{q} q \rangle \langle g_s^2 GG \rangle}{18\sqrt{2}} \left(\frac{1}{p^4} + \frac{1}{k^4} \right) \right).$$

$$-g_{\rho\pi} \frac{f_{\pi_1} f_\rho m_\rho f'_\pi}{m^2_\rho - m^2_{\pi_1}} \left(e^{-m^2_{\pi_1}/T^2} - e^{-m^2_\rho/T^2} \right) = -\frac{2\langle g\bar{q}\sigma G q\rangle}{3\sqrt{2}} - \frac{\langle \bar{q} q \rangle \langle g_s^2 GG \rangle}{9\sqrt{2}} \frac{1}{T^2}.$$

$$g_{\rho\pi} = 4.08^{+2.40}_{-1.83} \text{ GeV}^{-1},$$

$$\Gamma_{\pi_1 \to \rho\pi} = 242^{+310}_{-179} \text{ MeV}.$$

Decay behavior

B. Abnormal decay process $\eta_1 \equiv |\bar{s}sg; 0^{+}1^{-+}\rangle \to \eta\eta'$,

three-point correlation function:

$$T'_{\mu\nu}(p,k,q) = \int d^4x e^{-ikx} \langle 0|\mathbb{T}[J^{\mu}_{1-+}(0) J^{\eta\dagger}_{\nu}(x)]|\eta'\rangle \,, \qquad J^{\mu}_{1-+} \to \bar{s}_a \lambda^{ab}_n \gamma_\beta s_b g_s G^{\mu\beta}_n \,.$$

phenomenological side

$$T'_{\mu\nu}(p,k,q) = g_{\eta\eta'} k_\mu k_\nu \frac{f_{\eta_1} g_\eta}{(m^2_{\eta_1} - p^2)(m^2_\eta - k^2)} \,,$$

QCD side

$$\begin{aligned} & T'_{\mu\nu}(p,k,q) \\ = \; & \theta_s k_\mu k_\nu \left(- \frac{2m^2_{\eta'} f_{\eta'}}{3k^2} - \frac{4\pi^2 m^2_{\eta'} f_{\eta'} m_s \langle \bar{s}s \rangle}{3k^6} \right) , \end{aligned}$$

$$\begin{aligned} & g_{\eta\eta'} \frac{f_{\eta_1} g_\eta}{m^2_{\eta_1} - m^2_\eta} \left(e^{-m^2_\eta / M^2_B} - e^{-m^2_{\eta_1}/M^2_B} \right) \\ = \; & \frac{2\theta_s m^2_{\eta'} f_{\eta'}}{3} + \frac{2\pi^2 \theta_s m^2_{\eta'} f_{\eta'} m_s \langle \bar{s}s \rangle}{3} \frac{1}{M^4_B} \,. \end{aligned}$$

$$\begin{aligned} g_{\eta\eta'} &= 3.08^{+1.30}_{-0.91} \text{ GeV}^{-1} \,, \\ \Gamma_{\eta_1 \to \eta\eta'} &= 5.0^{+4.6}_{-3.1} \text{ MeV} \,. \end{aligned}$$

Decay behavior

Channel	$\|\bar{q}qg;1^-1^{-+}\rangle$ $M=1.67^{+0.15}_{-0.17}$ GeV	$\|\bar{q}qg;0^+1^{-+}\rangle$ $M=1.67^{+0.15}_{-0.17}$ GeV	$\|\bar{s}sg;0^+1^{-+}\rangle$ $M=1.84^{+0.14}_{-0.15}$ GeV
$\pi_1/\eta_1 \to \rho\pi$	242^{+310}_{-179}	–	–
$\pi_1/\eta_1 \to b_1(1235)\pi$	$14.5^{+25.9}_{-13.9}$	–	–
$\pi_1/\eta_1 \to f_1(1285)\pi$	$35.9^{+53.9}_{-36.4}$	–	–
$\pi_1/\eta_1 \to \eta\pi$	$2.3^{+2.5}_{-1.2}$	–	–
$\pi_1/\eta_1 \xrightarrow{b} \eta\pi$	$57.8^{+65.0}_{-31.4}$	–	–
$\pi_1/\eta_1 \to \eta'\pi$	$0.43^{+0.50}_{-0.28}$	–	–
$\pi_1/\eta_1 \xrightarrow{c} \eta'\pi$	149^{+162}_{-78}	–	–
$\pi_1/\eta_1 \to a_1(1260)\pi$	–	$79.5^{+112.4}_{-74.9}$	–
$\pi_1/\eta_1 \xrightarrow{a} \eta\eta'$	–	$0.07^{+0.12}_{-0.07}$	$0.93^{+1.04}_{-0.69}$
$\pi_1/\eta_1 \xrightarrow{b} \eta\eta'$	–	$1.62^{+2.13}_{-1.61}$	$1.64^{+1.51}_{-1.01}$
$\pi_1/\eta_1 \xrightarrow{c} \eta\eta'$	–	$11.5^{+11.7}_{-11.5}$	$5.0^{+4.6}_{-3.1}$
$\pi_1/\eta_1 \to K^*(892)\bar{K} + c.c.$	$25.3^{+34.7}_{-24.7}$	$25.3^{+34.7}_{-24.7}$	$73.9^{+85.7}_{-58.0}$
$\pi_1/\eta_1 \to K_1(1270)\bar{K} + c.c.$	–	–	$14.6^{+19.8}_{-14.6}$
$\pi_1/\eta_1 \to K^*(892)\bar{K}^*(892)$	–	–	$0.08^{+0.39}_{-0.08}$
Sum	530^{+540}_{-330}	120^{+160}_{-110}	100^{+110}_{-80}

Outline

- Introduction
- Method of the QCD sum rules
- Numerical analyses
- Decay behavior
- **Summary**

Summary

- We calculate the masses of forty-four single-gluon hybrid states with the quark-gluon contents $\bar{q}qg$ ($q = u/d$) and $\bar{s}sg$.
- Our results support the interpretations of the $\pi_1(1600)$ and $\eta_1(1855)$ as the hybrid states $|\bar{q}qg;\ 1^-1^{-+}\rangle$ and $|\bar{s}sg;\ 0^+1^{-+}\rangle$, respectively.
- Considering the uncertainties, our results suggest that the $\pi_1(1600)$ and $\eta_1(1855)$ may also be interpreted as the hybrid states $|\bar{q}qg;\ 1^-1^{-+}\rangle$ and $|\bar{q}qg;\ 0^+1^{-+}\rangle$, respectively.
- To differentiate these two assignments and to verify whether they are hybrid states or not, we propose to examine the $a_1(1260)\pi$ decay channel in future experiments.

Thanks for your attention !